



## **Neuromuscular Junction Structural Characteristics in Familial ALS Mice Model**

**Hafiz Usman Ghani <sup>a\*</sup>, Rafi Ullah <sup>a</sup>, Muhammad Abbas <sup>b</sup>, Muhammad Fawad <sup>b</sup>  
and Liu Ya Ling <sup>c</sup>**

<sup>a</sup> Hebei Medical University, China.

<sup>b</sup> Hebei North University, China.

<sup>c</sup> 2<sup>nd</sup> Affiliated Hospital of Hebei Medical University, China.

### **Authors' contributions**

*This work was carried out in collaboration among all authors. All authors read and approved the final manuscript.*

### **Article Information**

DOI: 10.9734/JPRI/2022/v34i44A36336

### **Open Peer Review History:**

This journal follows the Advanced Open Peer Review policy. Identity of the Reviewers, Editor(s) and additional Reviewers, peer review comments, different versions of the manuscript, comments of the editors, etc are available here: <https://www.sdiarticle5.com/review-history/89039>

**Original Research Article**

**Received 03 May 2022**

**Accepted 08 July 2022**

**Published 12 July 2022**

## **ABSTRACT**

**Introduction:** Amyotrophic lateral sclerosis (ALS) is a fatal neurodegenerative disease that can cause motor neuron degeneration in the spinal cord and motor cortex. Although most cases of ALS are sporadic, copper-zinc superoxide dismutase-1 (SOD1) mutations are responsible for 10%-20% of familial ALS.

**Objective:** Studying neuromuscular junctions in various age groups to see how they vary in structure.

**Methods:** From male hemizygous carriers (B6SJL-Tg (SOD1-G93A) 1Gur/J) and female B6SJL/F1 hybrids, female G93ASOD1 transgenic mice and age-matched wild-type (WT littermate partners, both were purchased from Jackson) laboratory. The animals were kept in an environment with controlled humidity and temperature, and 12:12h light was performed in a dark schedule, and sterile rodent food and sterile food were provided without specific pathogens.

**Results:** WT and SOD1 are present in 40, 60, 90, 120 days of mice Inside the Tibialis anterior of G93ASOD1 mice (TA) and gastrocnemius (GN) construction. The neurofilament heavy polypeptide (tubulin, green) points to the presynaptic end.  $\alpha$ -Bungarotoxins (BTX, white) mark the postsynaptic space, and synaptophysin (p38-1, red) is used for synaptic vesicles. In the following research we demonstrate that in 40 days of mice WT and SOD1 neither of them degraded while in 60 days of mice a slight denaturation occur in WT and SOD1 Further in 90 days of mice the degeneration is not serious about 60% to 70%. Furthermore, the deterioration in mice after 90 days is only 60-70 percent significant.

**Conclusion:** NMJ innervation has appeared Disappearance, loss of motor axons, and huge structural damage to the NMJ at 60 and 90 days. Structural changes in presynaptic and postsynaptic structures and a gradual decrease in synaptic vesicles observe.

*Keywords: Amyotrophic lateral sclerosis; neuromuscular junction; synapse; SOD1.*

## 1. INTRODUCTION

“Amyotrophic lateral sclerosis (ALS) is a neurodegenerative disease characterized by the degeneration of motor neurons in the brain and spinal cord, as well as rapidly progressive muscular atrophy, weakness, and paralysis. Although most ALS cases are sporadic, approximately 10% are familial. Mutations in the gene that encodes for the superoxide dismutase 1 (SOD1) account for almost 20% of familial ALS and 5% sporadic ALS cases” [1,2]. “To date, the exact etiology of ALS remains unclear, and no therapy substantially improves patient outcomes. ALS clinically begins with local muscle weakness and gradually spreads to all the voluntary muscles. Typical muscle pathology includes denervated atrophy, as well as myopathic features” [3], muscle fibrosis, and inflammation [4,5]. “Skeletal muscle roughly accounts for 40% of the body lean mass, thereby effective mechanisms for recycling damaged or aged organelles and protein aggregates and endurance for meeting physical demands are required by this specific muscle group” [6]. “Proper autophagic flux is vital for maintaining skeletal muscle functions, including metabolism and movement. But impairment of autophagic flux likely results in muscle atrophy and degeneration through inflammation, oxidative stress, and abnormal mitochondrial degradation” [7-14]. “Functional motor recovery after peripheral nerve injury depends on two key factors: (1) nerve regeneration at the injury site; and (2) NMJ re-innervations within target muscle. The NMJ represents the interface of nerve and muscle and is composed of three main structures: the nerve terminal, which contains acetylcholine (ACh) vesicles to be released across the synaptic cleft; the motor endplate covered in acetyl- choline receptors (AChRs); and 3 to 5 nonmyelinating terminal Schwann cells (tSCs), or per synaptic Schwann cells, that encase the nerve terminal and synapse”. [15-17] “The NMJ is not a static structure as it undergoes continuous remodeling throughout the lifetime of the animal and after injury”. [16,17] “Whereas nerve regeneration at the injury site has been the primary subject of many investigations, the process of NMJ re innervations after nerve injury

is still incompletely characterized”. [18,19]. “Loss of NMJ is considered the first pathophysiological event in ALS and occurs from loss of the motor neuron axon resulting in loss of the post-synaptic apparatus” [20]. “mSOD1 models have revealed a number of presymptomatic changes, including vulnerability to environmental stresses such as hypoxia during the presymptomatic period” [21]. “Such environmental triggers have been demonstrated to act in multiple neuronal compartments, including the NMJ” [21]. “Murine models for peripheral motor neuropathy, bax deletion and mSOD1G93A have also indicated that the triggering and regulation of degeneration in ALS occurs in a compartmented manner, with prevention of somal degeneration rarely extending to protection of the distal axon or improvement in clinical outcomes” [22-24]. “Thus, degeneration of the distal components is a key process in ALS. However, the sequence of changes is not fully known. Furthermore, understanding the post-synaptic changes will help determine the role of muscle versus motor neuron in the mechanisms of degeneration of the NMJ” [25].

## 2. MATERIAL AND METHODS

From male hemizygous carriers (B6SJL-Tg (SOD1-G93A) 1Gur/J) and female B6SJL/F1 hybrids, female G93ASOD1 transgenic mice and age-matched wild-type (WT littermate partners, both are purchased From Jackson) laboratory. The animals are kept in an environment with controlled humidity and temperature, 12:12h light is performed in a dark schedule, and sterile rodent food and sterile food are provided without specific pathogenesis.

### 2.1 Muscle Harvest

At the allocated time-point (t = 40, 60, 90,120 days of the age), animals were anesthetized, and an - cut was made preposterous right leg reaching out from the dorsal foot to the knee. After recognizable proof, the distal ligament of the Tibialis anterior lis foremost (TA) and Gastrocnemius (GS) muscles was cut across. The TA and GS were then painstakingly taking apart proximally to abstain from tearing where

the part of the perennial nerve embeds. After analysis, the TA and GS muscles were taken out any trash or hair and promptly positioned on the gum Tragacanth(GT), then plunged for 10 to 15 seconds in the chilly 2-methylbutane(cold by fluid nitrogen). keep TA and GS muscles in the -20°C. Animals went through cervical separation under profound sedation. All animal experiments were carried out in accordance with the guidelines for the Management of experimental animals formulated by the Ministry of Science and Technology of the People's Republic of China and the internationally accepted guidelines issued by The National Institute of health.

Total RNA was extracted with Trizol and retro-transcribed using the Taqman reverse transcription kit (Servicebio; Cat.No: G3013) according to the manufacturer's protocol. qRT-PCR was performed using SYBR Green Master mix (ABI Cat. No: Stepone plus) following the manufacturer's instructions. Relative expression values were normalised to the housekeeping gene GAPDH. Primer sequences are listed in the table below.

Ultrathin sections (10µm) of all preparations were cut using a Leica Ultracet R microtome (Leica Microsystem, Austria) with a Diatom diamond knife (Diatomite. CH-2501 Biel, Switzerland) Serial transverse cryosections (10 µM) were fixed on glass slides (adhesion microscope slides) . Tissue were rinsed 3 x 10 minutes in PBS and permeabilized using 0.3% Triton-X-100 diluent for 15 minutes (Sigma -Alorich) with Tween (membrane antibodies do not require this step). Added 50ul the donkey serum for 50 minutes (as protocol). Primary antibodies were added at pre- determined concentrations and incubated at room temperature for 1 hour followed by overnight at 4°C; tissue was rinsed 3 x 10 minutes in PBS and put the secondary antibodies. Secondary antibodies were incubated for 2 hours at room temperature in the dark. Immediately following secondary antibody removal, tissue were counterstained using DAPI (4',6-Diamidino-2- Pheylindole).The following antibodies were used:Synaptophysin-1 (P-38 1:500 , cat.no;101022,poly clonal rabbit antibody,

37079 Göttingen Germany); Alpha Tubulin(tubulin 1:500, cat. no; 66031-1-ig,mouse monoclonal antibody, proteintech); α-Bungarotoxin(α-BTX 1:500,CF dye conjugates); goat anti-rabbit Alexa Fluor 488 (1:1000; Thermo Fisher; Cat. No: A- 11034); or goat anti-mouse Alexa Fluor 594 (1:1000; Thermo Fisher; Cat. No: A-11037). The nuclei were counterstained with DAPI Fluoromount-G (Southern Biotech). The slides were observed using a fluorescence confocal microscope (Olympus FV1000). The experimental setup includes the laser power value, HV, gain, and offset parameters for each channel, which are determined at the beginning of each individual imaging process (by evaluating the background reactivity and saturation level of each channel) and remain constant throughout the imaging process. The colocalisation channel was produced for each Z-stack and was quantified in Olivia based on the overlap. The percentage of positive cells was shown by the ratio of positive cells to DAPI at selecting five x 20 magnification fluorescence fields. The percentage of fibrosis area was accounted at five x 20 magnification fluorescence images. The experiments were repeated three times with 6 mice in each group. The Image-Pro plus 5.1 software was used to analyses the fluorescence quantification.

### 3. RESULTS

The results show that both WT and SOD1 are present in 40-day-old mice. Inside the Tibialis anterior of G93ASOD1 mice (TA) and gastrocnemius (GN) construction. The picture (below) shows the number of neuromuscular junctions (NMJ) in various gatherings. The neurofilament heavy polypeptide (tubulin, green) points to the presynaptic end. A-Bungarotoxins (BTX, white) mark the postsynaptic space, and synaptophysin (p38-1, red) is used for synaptic vesicles. The following results show that neither of them has degraded and is 90% complete while in 60 days mice the results showed that is WT and SOD1, the denaturation is about 70% to 80% which means that a slight denaturation has occurred on the other hand in 90 days of mice the degeneration is not serious is about 60% to 80%.

Gene symbol	Forward primer	Reverse primer
YH1	TTCAAGTTTGGACCCACGGT	TTCTGAGCCTCGATTGCTC
MYH2	TTTGCCAGTAAGGGTCTGTGAG	GCTCCGCCACAAAGACAGAT
MYH4	AAGCCTGCCTCCTTCTTCATC	CTTAGCATCCACCACAAACAC
MYH7	CCCAGAAACAAGTGAAGAGCCT	GTTCCACGATGGCGATGTTC
GAPDH	CCTCGTCCCCTAGACAAAATG	TGAGGTCAATGAAGGGGTCGT

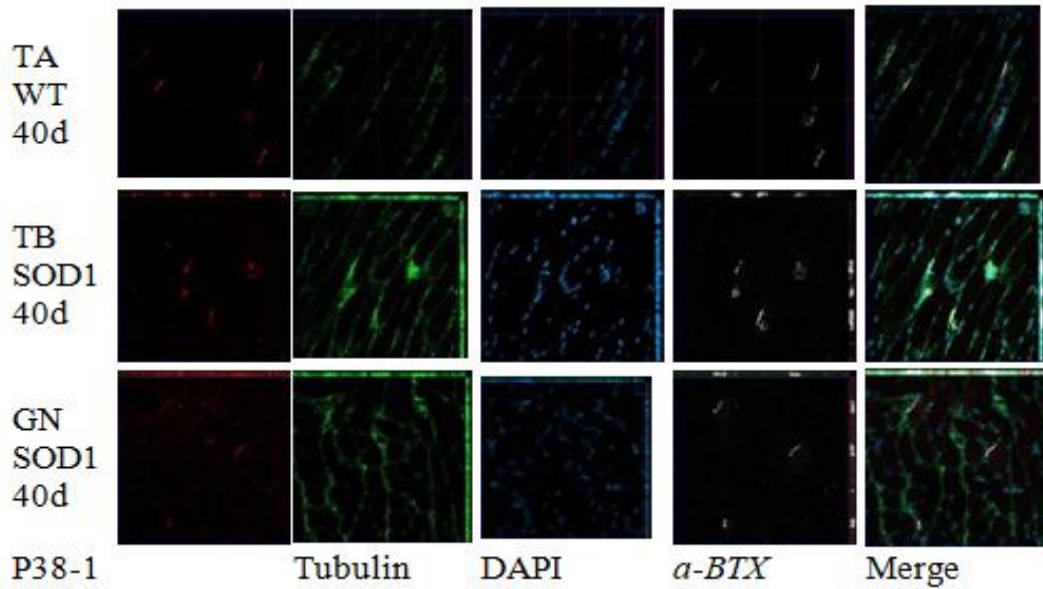


**Fig. 1.** 40-day-old mice have the WT and SOD1 genes. The gastrocnemius (GN) and Tibialis anterior (TA) of G93ASOD1 mice were constructed. The number of neuromuscular junctions (NMJ) in distinct groups is shown in the image (above). Presynaptic terminus is shown by the neurofilament heavy polypeptide (tubulin, green). BTX (white) and synaptophysin (p38-1, red) identify the postsynaptic space and synaptic vesicles, respectively

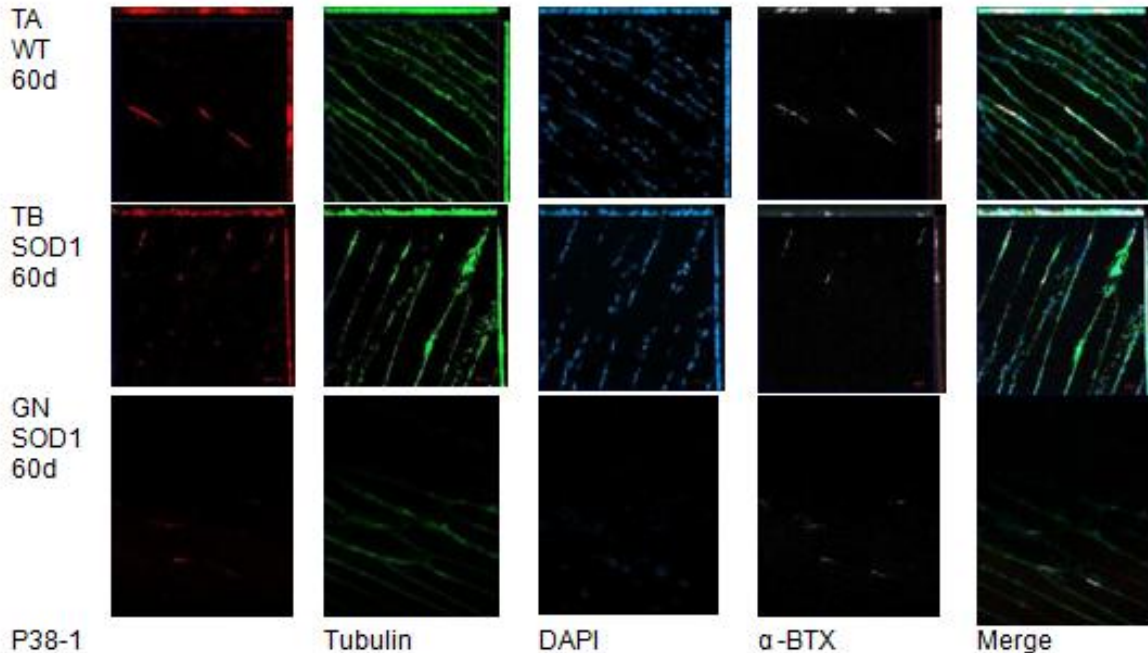


**Fig. 2.** 60-day-old mice have the WT and SOD1 genes. The gastrocnemius (GN) and Tibialis anterior (TA) of G93ASOD1 mice were constructed. The number of neuromuscular junctions (NMJ) in distinct groups is shown in the image (above). Presynaptic terminus is shown by the neurofilament heavy polypeptide (tubulin, green). BTX (white) and synaptophysin (p38-1, red) identify the postsynaptic space and synaptic vesicles, respectively

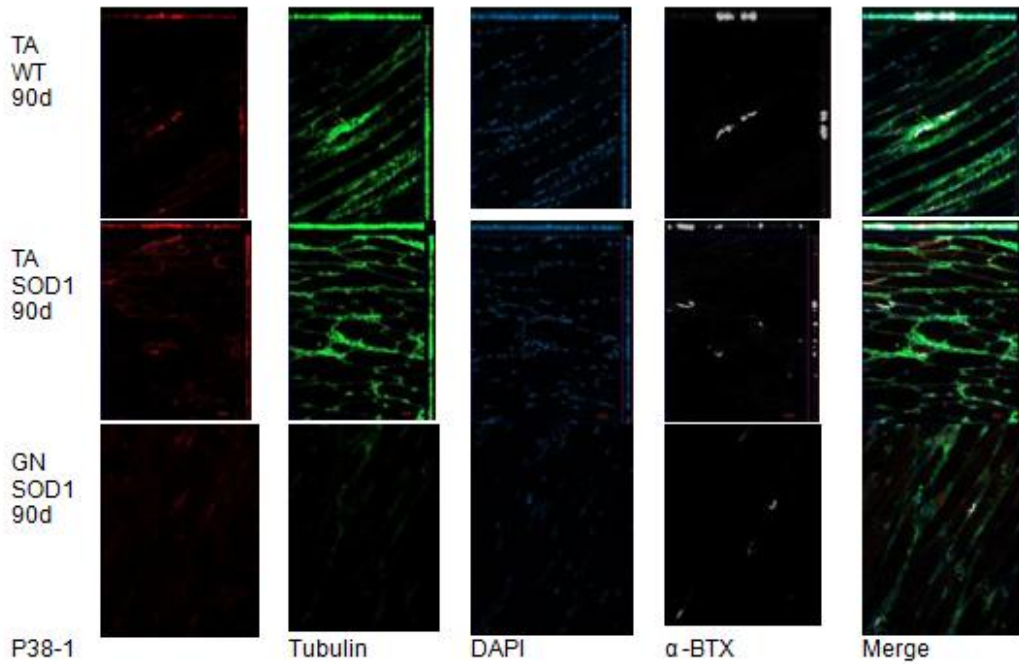


**Fig. 3.** Mouse strains that are 90 days old have both WT and SOD1. The gastrocnemius (GN) and Tibialis anterior (TA) of G93ASOD1 mice were constructed. The number of neuromuscular junctions (NMJ) in distinct groups is shown in the image (above). Presynaptic terminus is shown by the neurofilament heavy polypeptide (tubulin, green). BTX (white) and synaptophysin (p38-1, red) identify the postsynaptic space and synaptic vesicles, respectively

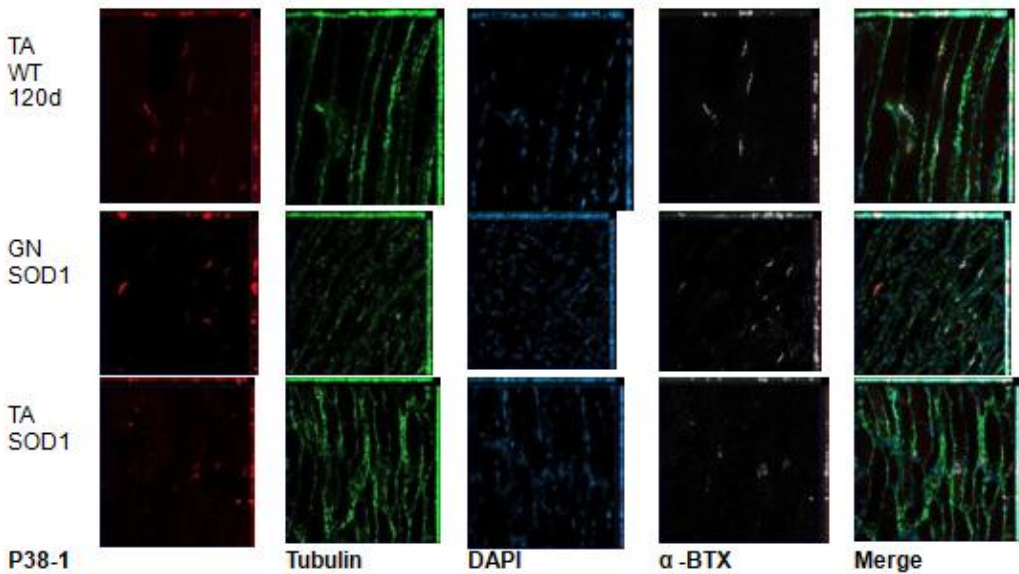


**Fig. 4.** WT and SOD1 are found in mice that are 120 days old. The gastrocnemius (GN) and Tibialis anterior (TA) of G93ASOD1 mice were constructed. The number of neuromuscular junctions (NMJ) in distinct groups is shown in the image (above). Presynaptic terminus is shown by the neurofilament heavy polypeptide (tubulin, green). BTX (white) and synaptophysin (p38-1, red) identify the postsynaptic space and synaptic vesicles, respectively

#### 4. DISCUSSION

In this study, after observing the structural characteristics of the neuromuscular junction in WT and SOD1 mice at 40, 60, 90 and 120 days, we concluded that at 40 days, NMJ innervation has appeared. Disappearance, loss of motor axons, and huge structural damage to the NMJ at 60 and 90 days. Based on our data, we observed structural changes in presynaptic and postsynaptic structures and a gradual decrease in synaptic vesicles. In this study, we have identified the basic molecular events of these systemic changes and provided experimental evidence for their feasibility as a drug target. The develop fiber sorts of mammalian skeletal muscles can be separated into two kinds: type 1 (moderate jerk) and type 2 strands (quick jerk). Type 2 strands can be additionally separated into type 2A (quick oxidative), type 2B (quick glycolytic), and type 2X (middle glycolytic) [26], which are encoded by MYH7 as a sluggish MYH quality and MYH1, MYH2, and MYH4 as quick MYH qualities [27]. Recovering muscles at first express undeveloped MyHCs, however before long begin to communicate grown-up quick MyHCs [28]. The change from early stage to grown-up quick myosins is free of innervations, while the progress from grown-up quick myosin to moderate myosin requires the contribution of the sluggish nerves [63]. The quick to-moderate change in the fiber type has been accounted for beforehand in ALS mice [29,30]. The sort progress towards quick or moderate fiber joined by re-innervations of recovering muscle was as yet questionable [31], albeit late proof had shown that the quick to-moderate shift might be an aftereffect of re innervations [32,33]. There is now growing consensus in the field that motor neurons are not the only primary target of SOD1, and increasing evidence indicates an involvement of NMJ destruction in aging-associated sarcopenia and in the pathogenesis and progression of neuromuscular diseases, including ALS [34,35,36,] However, controversy exists over whether NMJ dismantlement is a pathogenic event directly associated with the primary defects occurring in motor neurons or whether it occurs independently from motor neuron degeneration. To address this question, we made use of SOD1G93A mice (7) which represent an ideal model to separate the ubiquitous toxic effects of mutant SOD1G93A (10) with that of tissue-specific effects. In fact, the animal model that expresses the toxic mutant protein ubiquitously in all tissues, could not rule out which cell type, namely motor neurons or

muscle fibers, might initiate NMJ as consequence of oxidative damage caused by the toxic effect of SOD1. Despite numerous studies on motor neuron dysfunction in ALS, it is still debated whether motor neuron impairment in ALS has to be considered a dying forward phenomenon, in which primary damages occur in motor neurons in the cortex (i.e., through glutamate excitotoxicity or altered neuronal excitability) and then extend in an anterograde fashion to corticospinal projections or if ALS has to be considered a distal axonopathy in which motor neuron degeneration starts at the nerve endings and progress toward the cell bodies in a dying back manner[37,38] Given the complexity of ALS pathogenesis it is reasonable to consider that both dying forward and dying back processes can occur independently from each other and, regardless of the progression mode, it is acknowledged that disassembly of the NMJ, leading to skeletal muscle denervation, is a key point in ALS clinical symptoms onset and pathogenesis. The notion of ALS as a non-cell autonomous disease is based on the observation that, besides motor neurons, other cell types are damaged and display altered behavior both in patients and in vitro/in vivo models of ALS. Moreover, in the past fifteen years, this was shown by expressing ALS-linked mutant proteins in a tissue or in a cell-specific manner[39] While it is generally accepted that expression of ALS-linked mutated proteins in motor neuroses needed to induce an ALS phenotype in mouse models, it is still debated whether this is a sufficient condition. Initial studies on mice showed that neuron specific mutant SOD1 expression was not sufficient for the development of the disease [40,41]. This observation was confirmed by the generation of chimerical mice where it was shown that, in the absence of mutant SOD1 expression in non-neuronal cells, mutant SOD1 in neurons was not toxic in itself. On the other hand, a few years later it was reported that limited expression of mutant SOD1 in neurons was enough to induce an ALS phenotype in mice [34]. The reasons of this difference might be related to different expression levels of the transgenic in the different models. Overall, these studies define a scenario in which, in animal models, the expression of mutant SOD1 in neurons is crucial to determine the onset of the disease and the early phases of pathogenesis, whereas expression in non-neuronal cells is relevant to modulate ALS progression. When analyzing NMJ disassembly in ALS it is necessary to consider the specific role played by the three components

of the tripartite synapse in the series of events that culminate in muscle fiber denervation. Despite the wealth of data describing motor neuron degeneration during ALS pathogenesis, quite few studies addressed the changes occurring at the motor nerve endings at the NMJ.

## 5. CONCLUSION

In this study, after observing the structural characteristics of the neuromuscular junction of WT and SOD1 mice at 40, 60, 90 and 120 days, we concluded that at 40 days, the innervation of NMJ has disappeared. Loss of motor axons, NMJ huge structural damage occurred at 60 days and 90 days. Based on our data, we observed structural changes in presynaptic and postsynaptic structures and a gradual decrease in synaptic vesicles. In this study, we found that the delivery of neuromuscular junctions in ALS model mice SOD1-G93A has undergone basic structural changes. We have identified the basic molecular events of these systemic changes and provided experimental evidence for their feasibility as a drug target.

## ETHICAL APPROVAL

All animal experiments were carried out in accordance with the guidelines for the Management of experimental animals formulated by the Ministry of Science and Technology of the People's Republic of China and the internationally accepted guidelines issued by The National Institute of health.

## COMPETING INTERESTS

Authors have declared that no competing interests exist.

## REFERENCES

1. Wang Y, Bai L, Li S, Wen Y, Liu Q, Li R et al. Simvastatin enhances muscle regeneration through autophagic defect-mediated inflammation and mTOR activation in G93ASOD1 mice. *Mol Neurobiol.* 2020;1-14.
2. Rosen DR. Mutations in Cu/Zn superoxide dismutase gene are associated with familial amyotrophic lateral sclerosis. *Nature.* 1993;364(6435):362.
3. Iwasaki Y, Sugimoto H, Ikeda K, Takamiya K, Shiojima T, Kinoshita M. Muscle morphometry in amyotrophic lateral sclerosis. *Int J Neurosci.* 1991;58(3-4):165-70.
4. Jensen L, Jørgensen LH, Bech RD, Frandsen U, Schrøder HD. Skeletal muscle remodeling as a function of disease progression in amyotrophic lateral sclerosis. *BioMed Res Int.* 2016; 2016:5930621.
5. Al-Sarraj S, King A, Cleveland M, Pradat PF, Corse A, Rothstein JD et al. Mitochondrial abnormalities and low grade inflammation are present in the skeletal muscle of a minority of patients with amyotrophic lateral sclerosis; an observational myopathology study. *Acta Neuropathol Commun.* 2014;2 :165.
6. Neel BA, Lin Y, Pessin JE. Skeletal muscle autophagy: a new metabolic regulator. *Trends Endocrinol Metab.* 2013;24 (12):635-43.
7. Fan Z, Xiao Q. Impaired autophagic flux contributes to muscle atrophy in obesity by affecting muscle degradation and regeneration. *Biochem Biophys Res Commun.* 2020;525(2):462-8.
8. Fan Z, Wu J, Chen QN, Lyu AK, Chen JL, Sun Y et al. Type 2 diabetes-induced overactivation of P300 contributes to skeletal muscle atrophy by inhibiting autophagic flux. *Life Sci.* 2020;258 (undefined):118243.
9. Xiao Y, Ma C, Yi J, Wu S, Luo G, Xu X et al. Suppressed autophagy flux in skeletal muscle of an amyotrophic lateral sclerosis mouse model during disease progression. *Physiol Rep.* 2015;3(1).
10. Sadeghi A, Shabani M, Alizadeh S, Meshkani R. Interplay between oxidative stress and autophagy function and its role in inflammatory cytokine expression induced by palmitate in skeletal muscle cells. *Cytokine.* 2020;125:154835.
11. Doerr V, Montalvo RN, Kwon OS, Talbert EE, Hain BA, Houston FE et al. Prevention of doxorubicin-induced autophagy attenuates oxidative stress and skeletal muscle dysfunction. *antioxidants (Basel).* 2020;9(3):263:antiox9030263.P.
12. Ko FC, Abadir PM, Marx R, Westbrook R, Cooke CA, Yang H et al. Impaired mitochondrial degradation by autophagy in the skeletal muscle of the aged female interleukin 12 null mouse; 2016.
13. De Castro GS, Simoes E, Lima JDCC, Ortiz-Silva M, Festuccia WT, Tokeshi F et al. Human cachexia induces changes in

- mitochondria, autophagy and apoptosis in the skeletal muscle. *Cancers*. 2019;11(9).
14. Asami Y, Aizawa M, Kinoshita M, Ishikawa J, Sakuma K. Resveratrol attenuates denervation-induced muscle atrophy due to the blockade of atrogin-1 and p62 accumulation. *Int J Med Sci*. 2018;15(6):628-37.
  15. What is Normal? Neuromuscular junction reinnervation after nerve injury<sup>5</sup>, Bloch-Gallego E. Mechanisms controlling neuromuscular junction stability. *Cell Mol Life Sci*. 2015;72(6):1029-43.
  16. Wilson MH, Deschenes MR. The neuromuscular junction: anatomical features and adaptations to various forms of increased or decreased neuromuscular activity. *Int J Neurosci*. 2005;115(6):803-28.
  17. Deschenes MR. Motor unit and neuromuscular junction remodeling with aging. *Curr Aging Sci*. 2011;4(3):209-20.
  18. Cattin AL, Burden JJ, Van Emmenis L, Mackenzie FE, Hoving JJ, Garcia Calavia N, et al. Macrophage-induced blood vessels guide Schwann cell-mediated regeneration of peripheral nerves. *Cell*. 2015;162(5):1127-39.
  19. Cattin AL, Lloyd AC. The multicellular complexity of peripheral nerve regeneration. *Curr Opin Neurobiol*. 2016;39:38-46.
  20. Dupuis L, Loeffler JP. Neuromuscular junction destruction during amyotrophic lateral sclerosis: insights from transgenic models. *Curr Opin Pharmacol*. 2009;9(3):341-6.
  21. David G, Nguyen K, Barrett EF. Early vulnerability to ischemia/reperfusion injury in motor terminals innervating fast muscles of SOD1-G93A mice. *Exp Neurol*. 2007;204(1):411-20.
  22. Sagot Y, Tan SA, Bilbao FD, Aebischer P. Bcl-2 overexpression axonal degeneration disease prevents motoneuron cell body loss but not in a mouse model of a neurodegenerative. *J Neurosci*; 1995.
  23. Gould TW, Buss RR, Vinsant S, Prevette D, Sun W, Knudson CM et al. Complete dissociation of motor neuron death from motor dysfunction by Bax deletion in a mouse model of ALS. *J Neurosci*. 2006;26(34):8774-86.
  24. Dewil M, dela Cruz VF, Van Den Bosch L, Robberecht W. Inhibition of p38 mitogen activated protein kinase activation and mutant SOD1(G93A)-induced motor neuron death. *Neurobiol Dis*. 2007;26(2):332-41.
  25. Brettschneider J, Rudolph AC, Lee VM, Romanowski JQ, del Tredici K. Amyotrophic lateral sclerosis—A model of corticofugal axonal spread. Distal axon and neuromuscular junction degeneration in amyotrophic lateral sclerosis Braak, H. *Nat Rev Neurol*. 2013;9:708-14.
  26. Moloney EB, de Winter F, Verhaagen J. ALS as a distal axonopathy: molecular mechanisms affecting neuromuscular junction stability in the presymptomatic stages of the disease. *Front Neurosci*. 2014;8:252.
  27. Ilieva H, Polymenidou M, Cleveland DW. Non-cell autonomous toxicity in neurodegenerative disorders: ALS and beyond. *J Cell Biol*. 2009;187(6):761-72.
  28. Pramatarova A, Laganière J, Roussel J, Brisebois K, Rouleau GA. Neuron-specific expression of mutant superoxide dismutase 1 in transgenic mice does not lead to motor impairment. *J Neurosci*. 2001;21(10):3369-74.
  29. Lino MM, Schneider C, Caroni P. Accumulation of SOD1 mutants in postnatal motoneurons does not cause motoneuron pathology or motoneuron disease. *J Neurosci Off J Soc Neurosci*. 2002;22:4825-32. *Int. J. Mol. Sci*. 2017, 18, 2092 14 of 16.
  30. Clement AM, Nguyen MD, Roberts EA, Garcia ML, Boillée S, Rule M; et al. Wild type nonneuronal cells extend survival of SOD1 mutant motor neurons in ALS mice. *Science*. 2003;302(5642):113-7.
  31. Jaarsma D, Teuling E, Haasdijk ED, de Zeeuw CI, Hoogenraad CC. Neuron-specific expression of mutant superoxide dismutase is sufficient to induce amyotrophic lateral sclerosis in transgenic mice. *J Neurosci Off J Soc Neurosci*. 2008;28(9):2075-88.
  32. Clark JA, Southam KA, Blizzard CA, King AE, Dickson TC. Axonal degeneration, distal collateral branching and neuromuscular junction architecture alterations occur prior to symptom onset in the SOD1(G93A) mouse model of amyotrophic lateral sclerosis. *J Chem Neuroanat*. 2016;76(A):35-47.
  33. Foltz SJ, Modi JN, Melick GA, Abousaud MI, Luan J, Fortunato MJ et al. Abnormal skeletal muscle regeneration plus mild alterations in mature fiber type specification in Fktn-deficient

- dystroglycanopathy muscular dystrophy mice. PLOS ONE. 2016;11(1):e0147049.
34. Schiaffino S, Rossi AC, Smerdu V, Leinwand LA, Reggiani C. Developmental myosins: expression patterns and functional significance. *Skelet Muscle*. 2015;5:22.
35. Whalen RG, Harris JB, Butler-Browne GS, Sesodia S. Expression of myosin isoforms during notexin-induced regeneration of rat soleus muscles. *Dev Biol*. 1990;141(1):24-40.
36. Kalhovde JM, Jerkovic R, Sefland I, Cordonnier C, Calabria E, Schiaffino S et al. 'Fast' and "slow" muscle fibers in hindlimb muscles of adult rat's regenerate from intrinsically different satellite cells. *J Physiol*. 2005;562(3):847-57.
37. Broch-Lips M, Pedersen TH, Riisager A, Schmitt-John T, Nielsen OB. Neuro-muscular function in the wobbler murine model of primary motor neuronopathy. *Exp Neurol*. 2013;248:406-15.
38. Peggion C, Massimino ML, Biancotto G, Angeletti R, Reggiani C, Sorgato MC et al. Absolute quantification of myosin heavy chain isoforms by selected reaction monitoring can underscore skeletal muscle changes in a mouse model of amyotrophic lateral sclerosis. *Anal Bioanal Chem*. 2017;409(8):2143-53.
39. Mendler L, Pintér S, Kiricsi M, Baka Z, Dux L. Regeneration of reinnervated rat soleus muscle is accompanied by fiber transition toward a faster phenotype. *J Histochem Cytochem*. 2008;56(2):111-23.
40. Lee YS, Lin CY, Caiozzo VJ, Robertson RT, Yu J, Lin VW. Repair of spinal cord transection and its effects on muscle mass and myosin heavy chain isoform phenotype. *J Appl Physiol* (1985). 2007;103(5):1808-14.
41. Matsuura T, Li Y, Giacobino JP, Fu FH, Huard J. Skeletal muscle fiber type conversion during the repair of mouse soleus: potential implications for muscle healing after injury. *J Orthop Res*. 2007; 25(11):1534-40.

© 2022 Ghani et al.; This is an Open Access article distributed under the terms of the Creative Commons Attribution License (<http://creativecommons.org/licenses/by/4.0>), which permits unrestricted use, distribution, and reproduction in any medium, provided the original work is properly cited.

*Peer-review history:*

*The peer review history for this paper can be accessed here:*  
<https://www.sdiarticle5.com/review-history/89039>